**A DUST DEPOSITION CHAMBER FOR THERMAL INFRARED SPECTRAL ANALYSIS OF COATED ROCKS IN A SIMULATED AIRLESS BODY ENVIRONMENT.** C. R. Tinker[1] and T. D. Glotch[1], [1]Dept. of Geosciences, Stony Brook University, Stony Brook, NY (connor.tinker@stonybrook.edu).

**Background:** Although unknown thermal infrared (TIR) spectral data sets can often be matched to a linear combination of known laboratory end-member spectra, previous studies have shown that in a simulated asteroid environment (SAE) contextual characteristics such as particle size and visible albedo have interconnected effects on TIR spectra [1-3]. This is further demonstrated by apparent disconnects between the spectral and thermophysical properties of Bennu.

Bennu's moderate bulk thermal inertia ($310 \pm 70$ J $s^{-1/2}$ $K^{-1}$ $m^{-2}$) is consistent with a surface covering of mm- to cm- scale particulates [4], while Ryugu's slightly lower estimated thermal inertia (150-300 J $s^{-1/2}$ $K^{-1}$ $m^{-2}$) suggests the presence of 1 to 10 mm scale fines [5]. Contrary to these expectations, images of Bennu and Ryugu returned by the Origins, Spectral Interpretation, Resource Identification, and Security-Regolith Explorer (OSIRIS-REx) and Hayabusa2 missions respectively appeared to lack abundant fines but were dominated by decameter-scale boulders [6-9]. This is further complicated for the case of Bennu where the largest boulders on the surface counterintuitively exhibit the lowest thermal inertias [7]. Spectral data from the OSIRIS-REx Thermal Emission Spectrometer (OTES) indicates Bennu may in fact contain a fine particulate component in some regions [10]. These contradictions indicate that typical thermal models that relate thermal inertia to particle size for a uniform particulate regolith may not be appropriate for Bennu.

This study builds upon the interpretation by [7] that Bennu's low thermal inertia boulders may be explained by dust cover. If fine dust coatings are present on Bennu's large boulders it would result in a masking of higher thermal inertia signatures and a lower bulk thermal inertia. This is contradicted by thermal models that can assume a constant thermal inertia with depth and still provide a good fit to the OTES diurnal temperature curves [11]. Other thermal models have indicated that homogeneous dust layers as thin as 10-100 μm have the potential to mask thermal signatures and distort diurnal temperature variations in an identifiable way [12]. Although there is little spectral and thermophysical evidence for a large-scale homogeneous dust layer on Bennu, the effect of very thin and/or laterally discontinuous dust coatings on thermal models is not well constrained. Heterogeneous dust coatings could lower the observed thermal inertia of large boulders without significantly distorting global diurnal trends, leading to apparent contradictions between the bulk thermal inertia and estimated particle size. This presents the need for a comprehensive understanding of how dust coatings of various thicknesses can affect TIR spectral and thermophysical analyses in airless body environments.

**Dust Deposition Chamber:** Previous methods used to simulate dust deposition include sifting [13], alcohol suspension [14-15], lofting via compressed air [16-18], and mechanical agitation/settling [19]. The dust deposition chamber to be used in this study is based on the "Pigpen" chamber by [19-20], in which dust is mechanically agitated and then circulated with fans before settling in a controlled environment. Accuracy and repeatability are achieved through a low-cost design that leverages commercial off-the-shelf (COTS) components and additive manufacturing techniques. The chamber and its six subsystems are shown in Figure 1. The chamber sits on a utility cart that is modified to provide vibration reduction and surface leveling. The enclosure (1) is designed to hold laboratory $N_2$ at 1 atm, which will reduce unwanted electrostatic effects. The sample holder (2) is attached to the base of the enclosure by vibration reduction mounts, and it is enclosed in a cone to prevent early deposition of dust ejected by fan turbulence. The feed (3) utilizes a 3D printed auger with a low pitch to allow for the slow and consistent input of analog dust. All motorized components of the chamber are operated through repeatable cyclable programs, using an Arduino MEGA 2560 REV3 microcontroller and electronic speed controllers (ESCs) where necessary. The agitator (4) utilizes centrifugal force to distribute dust dropped onto a single area over the entire radius of the enclosure. Dust is then further distributed through lofting by six low-velocity computer fans (5). The deposition chamber will be tested for repeatability and control of dust layer thickness through optical measurement. Coating thicknesses will be measured relative to the sample holder mask at 50 locations using a WiTEC confocal microscope with a Z stage offering sub-micron focus precision.

**Methods:** Substrates and dust samples to be used for simulating uniform dust-coated surfaces are sourced from a bulk antigorite sample procured from Excalibur Mineral Corporation and heated for 24 hours at 600 °C. This Mg-rich serpentine is a major component of CM chondrite matrix and the heating amorphizes the sample to produce spectral features more similar to CM chondrites. Based on previous work and the known effects of visible albedo on TIR spectra, 11 vol.%

nanophase carbon black lamp will be mixed with the dust sample to achieve a visible albedo (~.04) like that of Bennu [21]. A mix of particulate (180-250 μm) and chip substrates will be coated with dust using the deposition chamber. The specific dust layer thicknesses of each sample will be determined following deposition control testing.

TIR (5-50 μm) spectra of each sample will be taken under SAE conditions (~330 K) relevant to Bennu. This will be done using the Planetary and Asteroid Regolith Spectroscopy Environmental Chamber (PARSEC) which is a custom planetary environmental chamber at Stony Brook University. PARSEC uses a Nicolet 6700 FTIR spectrometer to measure TIR emission under a vacuum better than $10^{-6}$ mbar. The samples will be optically measured after all spectra are taken to ensure the approach to vacuum did not significantly alter the dust coating. To understand the effects of heterogeneous dust coatings, the preceding methods will be reapplied with the addition of a deposition mask that enables control of the coating geometry. Two different discontinuous patterns to be used are checkerboards that cover 25% and 50% of the sample surfaces (Figure 2). The deposition masks are 3D printed and will be used for a total of 22 samples. These mask patterns allow for a better understanding of temperature distributions within dust layers and how these relate to the observed TIR spectra.

**Conclusion:** This work is critical to interpreting the TIR spectral and thermophysical properties of Bennu and will provide the first TIR laboratory spectra of discontinuous dust coated surfaces in an SAE. A custom-built dust deposition chamber will enable repeatable experimentation with dust coatings of various thicknesses and patterns. Contradictions presented by the spectral and thermophysical analysis of Bennu expose an inability of current models to account for a complex particulate variety and/or discontinuous dust cover. This work will address these disconnects within the context of Bennu while more broadly providing a framework for quantitative TIR spectral and thermophysical analyses of complex airless body surfaces.

**References:** [1] Shirley K. A. and Glotch T. D. (2019) *JGR Planets*, *124*, 970-988. [2] Breitenfeld L. B. et al. (2019) *LPSC,* #1866. [3] Glotch T. D. et al. (2018) *JGR*, *123*, 2467-2484. [4] Emery J. P. et al. (2014) *Icarus, 234,* 17-35. [5] Müller T. G. et al. (2017) *Astron. Astroph., 599,* A103. [6] Lauretta D. S. et al. (2019) *Nature, 568(7750),* 55-60. [7] DellaGiustina D. N. et al. (2019) *Nat. Astron., 3,* 341-351. [8] Sugita S. et al. (2019) *Science, 364,* eaaw0422. [9] Michikami T. (2019) *Icarus, 311,* 179-191. [10] Hamilton V. E. et al. (2019) *Nature Aston., 3,* 332-340. [11] Rozitis B. et al. (2019) *Aster. Sci.,* #2055. [12] Biele J. (2019) *Prog. Earth. Planet. Sci., 6,* 48. [13] Crisp J. and Bartholomew M. J. (1992) *JGR, 97,* 14691-14699. [14] Fischer E. M. and Pieters C. M. (1993) *Icarus, 102,* 185-202. [15] Singer R. B. and Roush T. L. (1983) *LPS,* 708-709. [16] Johnson J. R. et al. (2002) *JGR Planets, 107,* 5053. [17] Johnson J. R. and Grundy W. M. (2001) *Geoph. Res. Let., 28,* 2101-2104. [18] Wells E. N. et al. (1984) *Icarus, 58,* 331-338. [19] Graff T. G. et al. (2001) *LPSC,* #1899. [20] Graff T. G. (2003) *M. S. Thesis, 106 pp.,* ASU, Tempe, AZ. [21] Breitenfeld L. B. et al. (2020) *LPSC,* #1124.

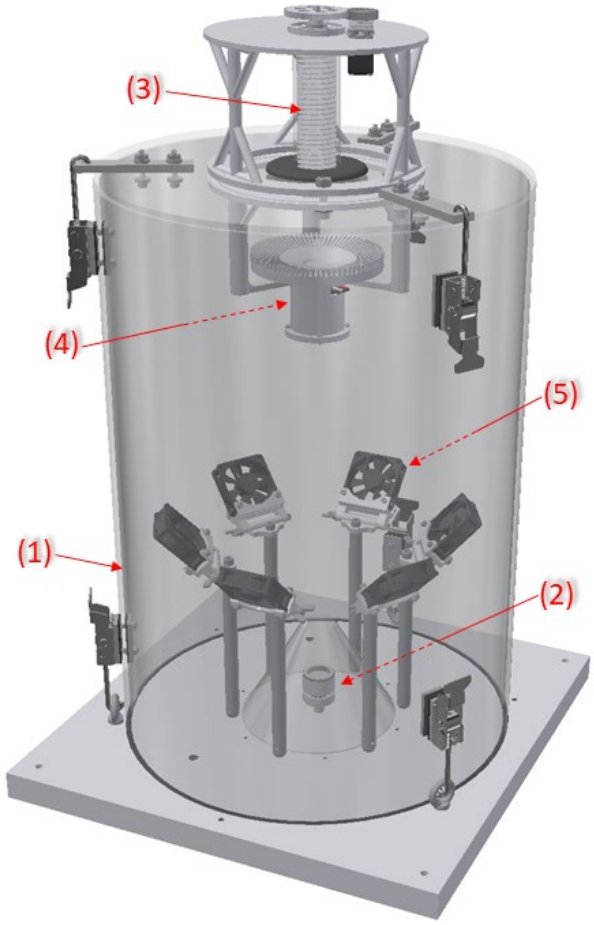


Figure 1: CAD rendering of the dust deposition chamber. Labeled subsystems include the enclosure (1), sample holder (2), feed (3), agitator (4), and distribution fans (5). The utility cart, electronics, and $N_2$ source are not shown.

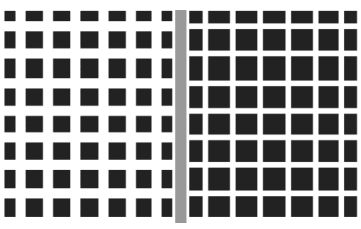

Figure 2: Example mask patterns for checkerboard dust deposition. Left: substrate 50% covered. Right: substrate 25% covered